AIAA JOURNAL
Vol. 37, No. 6, June 1999

Diode-Laser Sensors for Real-Time Control of Pulsed Combustion Systems

E. R. Furlong,* R. M. Mihalcea,† M. E. Webber,† D. S. Baer,‡ and R. K. Hanson§
Stanford University, Stanford, California 94305-3032

A diode-laser based, closed-loop control system has been developed to nonintrusively optimize a pulsed, 50-kW dump combustor. The adaptive control system used temperature and water mole fraction measurements obtained at 10-kHz rates from the peak absorbance values of H_2O features near 1.4 μm. In addition, measurements of CO, C_2H_2, and C_2H_4 concentrations in the exhaust, determined from diode-laser absorption spectra recorded using a fast-sampling probe and a multipass absorption cell (nominal 33-m-long path), were used to evaluate the effectiveness of the control strategies. A correlation was established between the magnitude of the observed temperature oscillations and the measured CO concentration in the exhaust. Adaptive control strategies were then applied to maximize the coherence of the burning vortices in the combustion region and thus optimize the combustor performance. The closed-loop control system was able to adaptively tune the phase and amplitude of the applied forcing within 100 ms and the forcing frequency within 10 s. These results demonstrate the applicability of multiplexed diode-laser absorption sensors for rapid, continuous measurements and control of multiple flowfield parameters, including trace species concentrations, in high-temperature combustion environments.

Nomenclature

A_{air}	= amplitude of secondary air forcing
f_0	= driving frequency
T_{f0}	= estimate of amplitude at f_0
T_{rms}	= 1 s rms amplitude at f_0
θ_{air}	= phase of secondary air forcing
τ_{act}	= characteristic actuator delay time
τ_{adapt}	= adaptation time
ϕ	= equivalence ratio

Introduction

NONINTRUSIVE measurements of multiple flowfield parameters have been demonstrated in a variety of flowfields using diode-laser absorption diagnostics.[1–6] Multiple diode lasers can be wavelength multiplexed by incorporating appropriate fiber splitters to combine the multiwavelength beam and enable the sensor system to access several species or different spectral regions of the same species simultaneously. These multispecies sensor systems can be used to measure temperature, pressure, and species concentrations at kilohertz rates along several paths simultaneously without increasing the number of laser sources.[7,8] Rapid measurements of important combustion parameters combined with a reliable closed-loop control strategy offer potential for significant improvements in combustion efficiency and reduced pollutant emissions.

In the present work a multiplexed diode-laser sensor system is applied to monitor and control a 50-kW combustor, which serves as a model of an afterburner in a waste incineration system under development at the U.S. Naval Air Warfare Center at China Lake, California, for use aboard Navy ships. The multistage incineration system converts solid waste to gaseous waste using a starved-air pyrolysis chamber and then removes the hazardous components using a secondary oxidation chamber or afterburner, which utilizes the concepts of forced vortex combustion for a compact and efficient design. Details of the afterburner, including the design, the application of advanced diagnostics, and the determination of the destruction and removal efficiency for both small- and large-scale systems have been described previously.[9–11]

A clean-burning, efficient, multistage incineration system must minimize effects caused by the time-varying flame speed, heat content, and flow rate from the pyrolysis chamber and the associated changes in the afterburner (combustor) dynamics. Adaptive, closed-loop control strategies[12,13] can compensate for these variations by continually adjusting appropriate system inputs (e.g., forcing amplitude, phase, and frequency) to optimize the combustor performance, provided effective sensors can be developed to accurately and reliably monitor the full range of anticipated flow conditions and appropriate system state parameters.

Sensors for real-time control must be capable of responding to the relevant timescales of complex combustion flows. Radiative emission[14–16] (including CH, OH, CO, soot) and pressure[17–20] sensors have been used extensively in real-time control systems because of their response time, compact size, and relative ease of use. Many laser-based strategies, although useful in analytical laboratory studies, use inefficient pulsed lasers that are large, expensive, and difficult to operate in real-time control applications. Diode-laser absorption sensors, in contrast, are relatively inexpensive, easy to use, easily coupled to optical fibers for remote probing of hostile environments, and may be applied to yield rapid, nonintrusive absolute measurements of important flow parameters.[1–6,21] In the context of waste incineration, diode-laser sensors offer the additional advantages that they require no calibration, are relatively unaffected by changes in the composition of the fuel, and are not subject to the harsh, corrosive environment present inside the combustion chamber.

In the present work diode-laser sensors and adaptive control strategies were applied to measure and control the coherence of vortices and extent of reaction in the combustion region while monitoring the CO and various unburned hydrocarbon (UHC) concentrations in the exhaust region.

Theory

The theoretical basis for determining gas temperature and species concentration from measured absorption spectra recorded in combustion flows[22] and the spectroscopic parameters of the H_2O

Presented as Paper 98-3949 at the AIAA/ASME/SAE/ASEE 34th Joint Propulsion Conference, Cleveland, OH, July 13–15, 1998; received Aug. 10, 1998; revision received Jan. 4, 1999; accepted for publication Jan. 19, 1999.

*Research Associate, High Temperature Gasdynamics Laboratory, Department of Mechanical Engineering; currently Mechanical Engineer, General Electric Company, Corporate Research and Development, One Research Circle, Bldg. K1-ES, Room 109, Niskayuna, NY 12309. Member AIAA.

†Research Associate, High Temperature Gasdynamics Laboratory, Department of Mechanical Engineering. Student Member AIAA.

‡Senior Research Scientist, High Temperature Gasdynamics Laboratory, Department of Mechanical Engineering. Member AIAA.

§Professor, High Temperature Gasdynamics Laboratory, Department of Mechanical Engineering. Fellow AIAA.

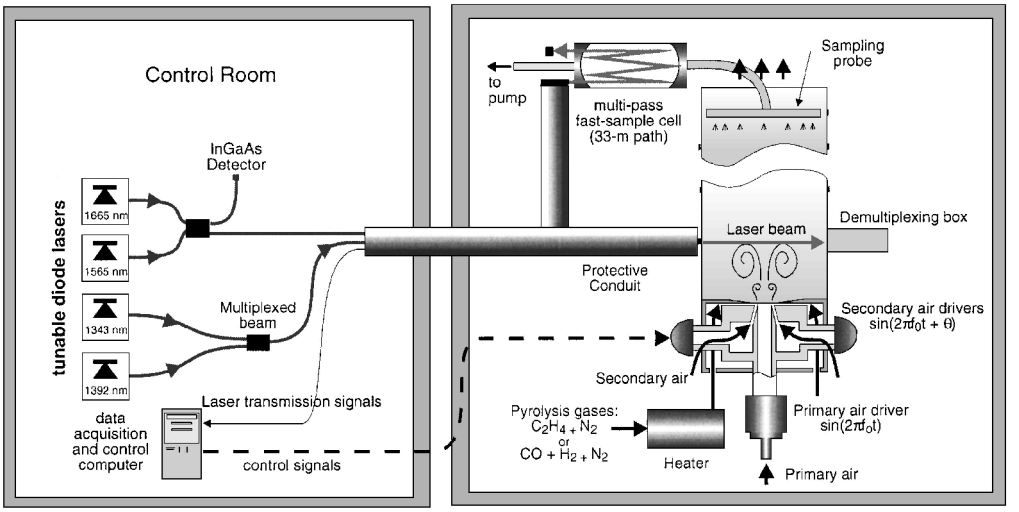

Fig. 1 Schematic diagram of the combustion-control experiment.

transitions (near 1343 and 1392 nm) and CO transitions (1568 nm) probed[23,24] have been described previously.[1–3,7,8] In brief, the gas temperature is determined from the ratio of measured H_2O absorbances obtained by tuning the narrow-bandwidth diode lasers across transitions near 1343 nm ($\nu_1 + \nu_3$ band) and 1392 nm ($2\nu_1, \nu_1 + \nu_3$ bands). The mole fractions (or concentrations) of probed species are determined from the measured absorbances at appropriate wavelengths using the known absorption line strengths at the measured temperatures.

Experimental Method

Figure 1 shows the general arrangement of the diode-laser sensors and the incinerator (afterburner) facility. Details of the afterburner operation can be found in Ref. 9. The primary airflow (900 l/min) through the central jet (3.84-cm diam) was acoustically forced (up to 100% rms) to create coherent vortices at the preferred mode of the jet. Secondary airflow (180 l/min) was acoustically modulated (near 100% rms) and injected circumferentially at a 15-deg angle relative to the primary air. The pyrolysis surrogate (355 l/min N_2 and 43 l/min C_2H_4; or 355 l/min N_2, 123 l/min CO, and 180 l/min H_2) was preheated to near 900 K and circumferentially injected normal to the primary airflow. The temperature of the pyrolysis surrogate was typically 600 K at the injection point. A water-cooled aluminum duct (18-cm diam, 61-cm length) was sealed to the injection nozzle.

The laser system includes two independently operated distributed-feedback (InGaAsP) diode lasers tuned at a 10-kHz repetition rate over the desired transitions by ramp modulating the individual injection currents to yield single-sweep spectrally resolved absorption records every 100 μs. The individual laser outputs were combined into a single path using appropriate single-mode fiber splitters and couplers. The multiwavelength beam was brought to the incinerator via an optical fiber encased in a protective conduit and directed through the flowfield using a gradient index lens (0.25 pitch, 3-mm diam). The transmitted multiwavelength light was demultiplexed (spectrally separated) into the constituent laser wavelengths by directing the beam at a non-normal incidence angle onto a diffraction grating (1200 g/mm, $\lambda_b = 1.0\,\mu$m). The beams were diffracted at angles specific to each wavelength and were subsequently monitored with InGaAs photodiodes (500-kHz bandwidth, 2-mm diam). The detector voltages were digitized by a 12-bit A/D card installed in a Pentium-based personal computer. The measurement cycles were repeated at a 3-kHz rate (each required 200μs for data transfer and 100 μs for signal acquisition and computation of gas temperature, water mole fraction, and control signal). The relatively short delay between the measurement and the subsequent control output (0.4 ms) was approximately 10 times shorter than the effective response time of the actuator ($\tau_{act} =$ 5 ms), which was limited by the gas-flow time to the probed region.

A water-cooled, stainless-steel probe (4.1-mm i.d.) with 13 0.7-mm-diam inlet holes was used to continuously sample combustion products for investigation with a multipass cell. The extracted gas was cooled, dried, and filtered to preserve the integrity of the silver-coated mirrors. Differential absorption spectroscopy techniques were used to determine absolute species (CO, C_2H_2, and C_2H_4) concentrations by tuning the wavelength of the lasers across transitions near 1646 nm ($\nu_1 + \nu_9$, $\nu_5 + \nu_9$ bands of C_2H_4), the R(13) transition of CO (3ν band) near 1564 nm, and the P(17) transition of C_2H_2 near 1535 nm ($\nu_1 + \nu_3$ band). The absorption measurements were recorded in a multipass cell (0.3-l volume, 3300-cm nominal path length) to increase measurement sensitivity.[25]

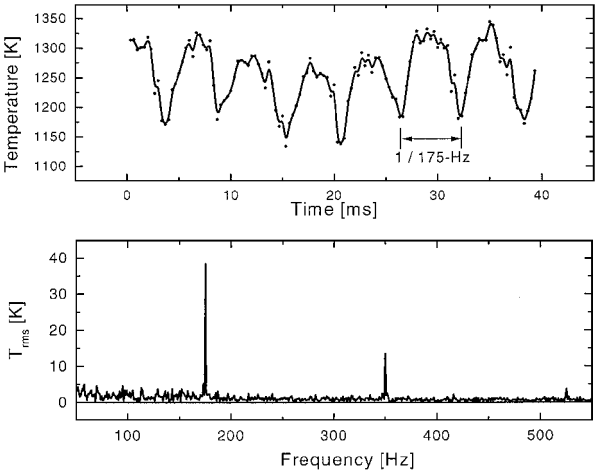

Fig. 2 Temperature measured at 3-kHz rate, 8 cm from the dump plane, using the C_2H_4–N_2 mixture (top panel). Power spectral density (1-Hz resolution) of a 1-s history of temperature measurements (bottom panel).

Combustion Measurements

Figure 2 (top panel) shows a time history of temperature measurements recorded at a 3-kHz rate 8 cm from the dump plane. The large periodic oscillations at the forcing frequency ($f_0 = 175$ Hz) are suggestive of strong coherent vortices and a proper relative phase between the primary and secondary air forcing. The power spectral density of the measured temperature (lower frame) confirms that the temperature oscillations are a result of the applied forcing. In the present work the rms magnitude of the spectral component near 175 Hz (the forcing frequency) was used as a measure of coherence. For the case of optimized forcing (Fig. 2), $T_{rms} = 38$ K. No effort was made in this work to control the higher-order modes visible in Fig. 2.

Figure 3 shows the measured changes in the normalized values of T_{rms} (measured 8 cm from dump plane) and CO concentration (measured from gases sampled 45 cm from dump plane) as the

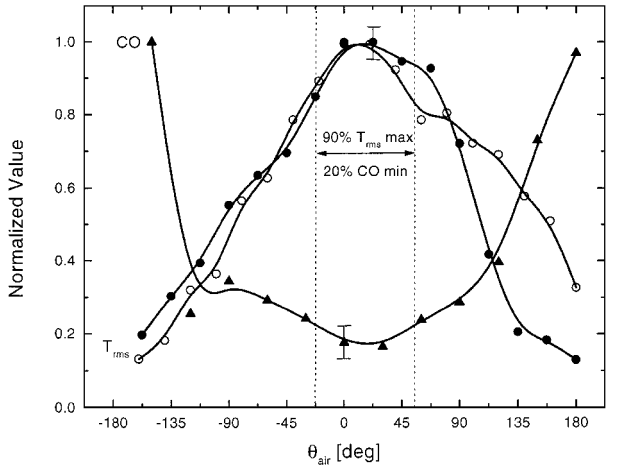

Fig. 3 Variation in rms temperature at f_0 (T_{rms}; ●, C_2H_4–N_2; ○, CO–H_2–N_2) and [CO] (▲, C_2H_4–N_2) with relative phase of primary and secondary air θ_{air}. Normalization values are T_{rms} = 34 K (●), T_{rms} = 16 K (○), and [CO] = 540 ppm. Steady parameter are $\phi = 0.575$ and f_0 = 175 Hz. The error bars reflect both the accuracy of the measurement and the repeatability of the operational conditions.

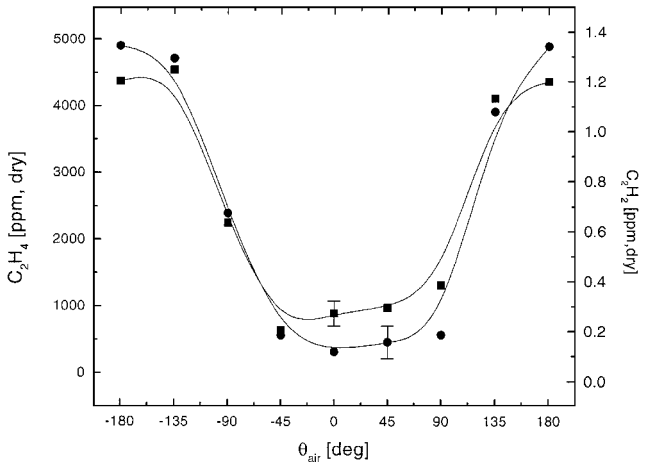

Fig. 4 Variation in [C_2H_4] (●) and [C_2H_2] (■), with relative phase of primary and secondary air, measured from gases sampled 27 cm from the dump plane. Steady parameters are $\phi = 0.575$ and f_0 = 175 Hz. The error bars reflect both the accuracy of the measurement and the repeatability of the operational conditions.

relative phase between the electric signals modulating the primary and secondary air was varied. The solid points correspond to the C_2H_4–N_2 mixture and the open points to the CO–H_2–N_2 mixture; the normalization parameters are indicated in the figure caption. The vertical dotted lines bound the phase values where the CO concentration is within 20% of the minimum (and the T_{rms} is within about 10% of the maximum) and indicate a measure of performance (open-loop operational boundaries) for the closed-loop control strategies. The strong correlation between high T_{rms} values and low CO levels confirms that flowfield coherence is a good indicator of combustor performance, which allows the use of fast, nonintrusive T_{rms} measurements for active control. The smaller T_{rms} values measured in the CO–H_2–N_2 mixture may indicate that H_2 combustion was occurring closer to the dump plane, reducing the energy content of the vortices. This occurrence was confirmed by time-averaged measurements of H_2O mole fraction, which showed significantly more variation with phase for the C_2H_4–N_2 mixture than the CO–H_2–N_2 mixture.

The variation in measured hydrocarbon emissions with phase, sampled 27 cm from the dump plane, is shown in Fig. 4 for the C_2H_4–N_2 fuel mixture. The similarity of the CO curves of Fig. 3 and the UHC curves in Fig. 4 confirms that there are no anomalies in the optimal forcing conditions (e.g., wall quenching) that might cause reduced CO levels but increased UHC levels. These results are

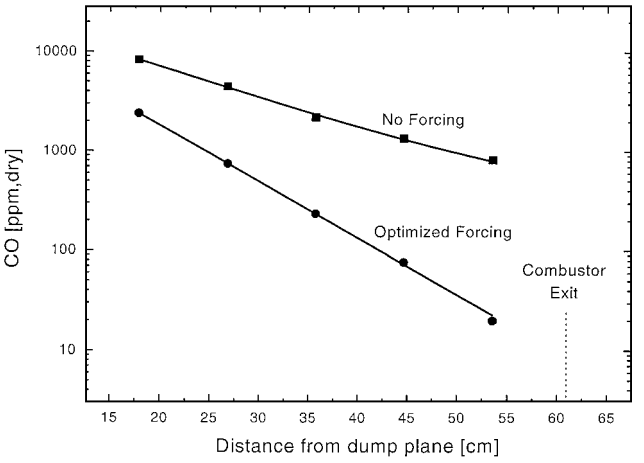

Fig. 5 Variation in measured CO levels with sampling location for the C_2H_4–N_2 mixture.

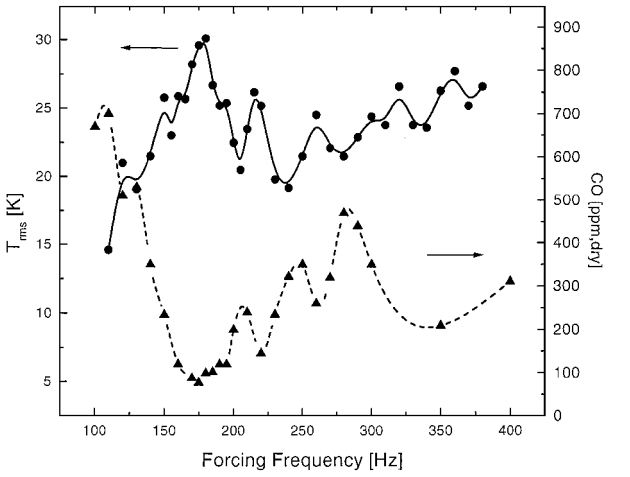

Fig. 6 Measured variation in T_{rms} and CO levels with forcing frequency for the C_2H_4–N_2 mixture.

also consistent with previous measurements, which showed that CO concentration was the lowest at the phase angle that most efficiently removed benzene.[9] Thus a measurement of CO can serve as an indicator of overall combustor performance. Neither C_2H_4 nor C_2H_2 were detected in the CO–H_2–N_2 mixture.

In the absence of forcing, the CO concentration decreased exponentially with downstream distance, as indicated in Fig. 5, for the C_2H_4–N_2 mixture. Measurements of the UHC indicated similar performance. The CO levels decreased monotonically with increasing actuator power until the power limit on the actuators was reached. With the application of optimized forcing, the CO levels are substantially lower and follow a steeper exponential trend. These curves demonstrate the importance of residence time in the destruction of CO and show how the forced-vortex concept can substantially reduce the necessary size (length) of the combustor.

The combustor is expected to operate most efficiently at the preferred mode of the primary air inlet. For a constant Strouhal number ($Sr \approx 1$) the frequency of this mode should scale with the flow rate of the primary air, that is, the optimal frequency should decrease from ~180 Hz at 900 l/min to ~140 Hz at 700 l/min. Competing resonances, which can interfere with (or "dephase") the forced oscillations, arise from both the secondary acoustic drivers, the nozzle geometry, and the various combustor modes. This mode competition can lead to a complicated frequency response and favor forcing frequencies other than the preferred inlet mode.

The variation in T_{rms} and CO levels with the forcing frequency is shown in Fig. 6 for the C_2H_4–N_2 mixture. For this condition, the optimal forcing is near 175 Hz. When the flow rates were lowered at a constant equivalence ratio, the optimal forcing frequency shifted toward lower frequencies (to approximately 140 Hz), as

expected. However, when the fuel composition was changed to CO–H_2–N_2, the optimal forcing frequency was no longer consistently near 175 Hz. For this fuel mixture the optimum was found to vary between local maxima at 183, 205, and 220 Hz. This unexpected shift signifies that in field operation, when the fuel mixture supplied to the incinerator will vary with time, the optimum forcing frequency should also be expected to vary. Any control strategy, though, must be robust enough to account for the complicated structure exhibited in Fig. 6, which is a result of the complex and time-varying interaction between the different combustor modes.

Closed-Loop Control

Closed-loop control was used to optimize the coherence of the oscillations by first varying the phase and amplitude of the secondary air forcing. Once the timescales required for phase optimization were understood, a second control strategy was implemented to concurrently adjust the forcing frequency in a concerted effort to maximize the amplitude of the forced oscillations.

First Control Strategy

The objective of the first control strategy was to maximize the magnitude and coherence of oscillations at the forcing frequency. Most of the energy associated with producing the vortices is supplied by the modulation of the primary air. The aim of the secondary forcing is to help entrain fuel into the vortex roll up, as the high strain rates in the vortex both enhance the mixing and delay the onset of combustion. As such, the secondary forcing is expected to augment the temperature oscillations measured when only the primary air is modulated. Therefore, a sinusoidal response, adjusted by a characteristic delay time τ_{act} to be in-phase with the air forcing, is defined to be the desired response. In general,

$$T_{desired}(t) = T_{mean,des} + T_{f_0,des}\sin[2\pi f_0(t - \tau_{act})] \quad (1)$$

where $T_{mean,des}$ is the desired mean temperature, $T_{f_0,des}$ is the desired level (amplitude) of oscillations (set at 40 K in the present experiments), and τ_{act} is the characteristic delay time of the actuator (5 ms). Defining the desired response will enable control decisions to be made after each measurement instead of waiting to accumulate enough data for a representative power spectral density. Furthermore, slight adjustments to the actuators can be made to counteract dephasing events in the combustor.

In previous work a fast-flow controller was used to stabilize the mean temperature over timescales on the order of τ_{act} (Ref. 26). In the present investigation, however, only the f_0 component of T was optimized. For applications in which minimum temperature oscillations are desired (e.g., to reduce fluctuations or instabilities in the combustor), $T_{f_0,des}$ can be set to zero.[27,28]

Several adaptive filter structures have been identified in the literature[12,13] and implemented on laboratory-scale combustors.[16,18–20] The adaptation in the present strategy implemented the least-mean-squared (LMS) algorithm.[12] LMS was first used to filter the temperature measurements by decomposing the time-domain temperature into its three largest components in the frequency domain (i.e., the mean value T_{mean}; the component at f_0, T_{f_0}; and the component at $2f_0$, T_{2f_0}) as

$$T \approx T_{mean} + T_{f_0}\sin\left(2\pi f_0 t - \theta_{f_0}\right) + T_{2f_0}\sin\left[2\pi(2f_0)t - \theta_{2f_0}\right] \quad (2)$$

The magnitudes (T_{mean}, T_{f_0}, T_{2f_0}) and phases (θ_{f_0}, θ_{2f_0}) were adaptively varied to follow closely the measured temperature and isolate the oscillations at the forcing frequency. This algorithm was similar to a variable frequency bandpass filter with a very small group delay. The ability to quickly adjust the frequency was used in the second control strategy, which will vary the forcing frequency.

The estimate of the oscillations at the forcing frequency was then used to evaluate the error, defined as the difference between the measured and desired reponses, given by

$$\varepsilon_T = T_{f_0,des}\sin[2\pi f_0(t - \tau_{act})] - T_{f_0}\sin\left(2\theta f_0 t - \theta_{f_0}\right) \quad (3)$$

The LMS algorithm then used a stochastic estimate of the performance gradient to vary θ_{air} and A_{air} and minimize this error. The new values of θ_{air} and A_{air} were computed according to the coupled, nonlinear relations

$$\theta_{air,new} = \theta_{air,old} - (C/\tau_{adapt})\varepsilon_T A_{air,old}\cos(2\pi f_0 t + \theta_{air,old}) \quad (4)$$

$$A_{air,new} = A_{air,old} + (C/\tau_{adapt})\varepsilon_T \sin(2\pi f_0 t + \theta_{air,old}) \quad (5)$$

where C is a unit-normalization constant and τ_{adapt} is the adaptation time. The new calculated phase and amplitude values were sent to the secondary air speakers every measurement cycle, i.e., at a 3-kHz rate.

To counteract the effects of dephasing (and minimize the response time), τ_{adapt} should be small. However, if τ_{adapt} is smaller than τ_{act}, the system can become unstable. Thus, as a compromise between accuracy and stability, the adaptation time was $\tau_{adapt} = 5\tau_{act}$ or 25 ms.

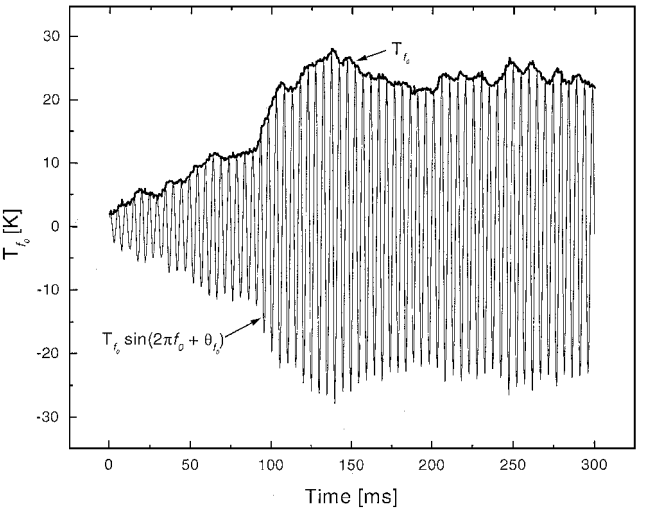

Fig. 7 Overall response time of the first control strategy. The component at the forcing frequency, as determined by the decomposition algorithm, grows as the control converges.

The ability of the control strategy to increase the amplitude of the temperature oscillations is shown in Fig. 7. Here the decomposition algorithm [Eq. (2)] is used to track the growth of the component at the forcing frequency as control is applied. The amplitude is shown as the bold envelope. The control was applied to the CO–H_2–N_2 mixture with an adaptation rate of 25 ms, a forcing frequency of 205 Hz, and a desired oscillation level of 40 K.

The internal variables associated with the control are shown in Fig. 8. The control was started with the phase at 180 deg, which was near a performance minimum in the open-loop experiments. The amplitude (bottom frame, right axis) at first decreased but then quickly increased to the power limit as the phase began to converge (bottom frame, left axis). Note that the phase reached the open-loop operational bounds (i.e., anticipated CO levels within 20% of the minimum) within approximately 100 ms. As the oscillations grew in phase with the primary air forcing (top frame, left axis), the error signal (temporally averaged magnitude) begins to decrease, indicating convergence (top frame, right axis).

To illustrate the effect of the adaptation time on coherence (Fig. 9), τ_{adapt} was increased from 25 ms (bottom panel) to 250 ms (top panel). The large variations in the measured coherence in the top frame are attributed to the complex interactions between the inlet mode, the combustor modes, and the preferred mode of the jet.[10] With faster adaptation the control system was able to compensate for some dephasing in the combustor, thereby both increasing and stabilizing the temperature oscillations. There was roughly a 10% increase in the T_{rms} value when the adaptation time was set at 25 ms.

The fast-sampling system was used to track the CO concentration as the control was applied and verify its effectiveness. A typical time-dependent CO measurement is shown in Fig. 10 for the CO–H_2–N_2 mixture. The transport time (~2.5 s) is associated with passage through the length of tubing between the sampling probe and the flow-through cell. The 1/e change-over time of the gases in the flow-through cell was approximately 1.1 s. The total flow-through time was then the combination of these two times and settled to

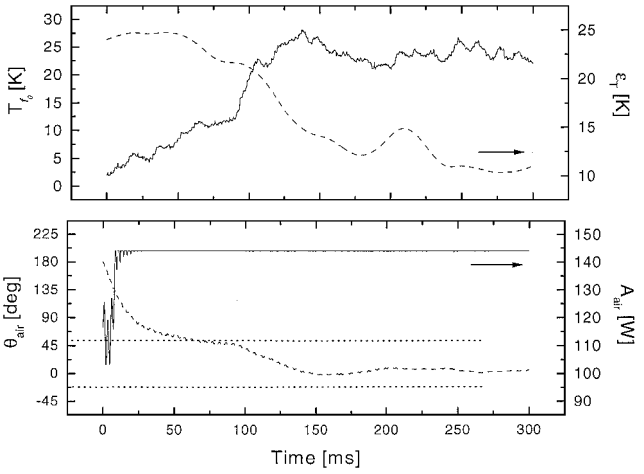

Fig. 8 Overall time response of the closed-loop system, which adaptively varied θ_{air} (bottom panel, left axis) and A_{fuel} (bottom panel, right axis) to minimize the error function, ε_T (top panel, right axis). Steady parameters are $\phi = 0.575$, $f_0 = 205$ Hz, and $T_{rms,des} = 40$ K. Horizontal dotted lines correspond to T_{rms} values greater than 90% of $T_{rms,max}$ in the open-loop experiments.

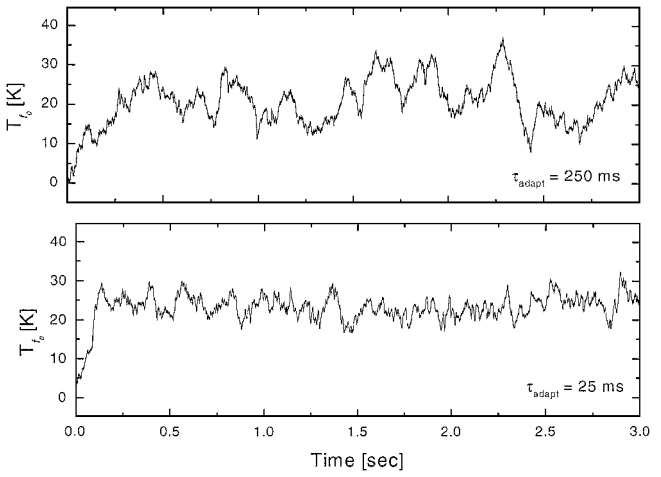

Fig. 9 Measured closed-loop performance for two different adaptation rates.

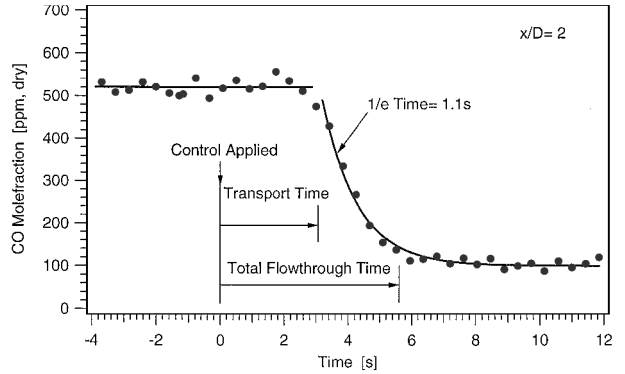

Fig. 10 Measured time history of CO concentration as control is applied.

within 10% of the final value after approximately 6 s. Because the laser tuning rate is much faster than the flow-through time, the C_2H_2 and C_2H_4 measurements are also flow limited and have the same response time as the CO measurements. The species selectivity, response time, and absolute nature of these measurements underscore the utility of diode-laser sensors for remote, continuous monitoring applications. Locating the cell closer to the combustor or using a cell with less volume can reduce the total flow-through time.

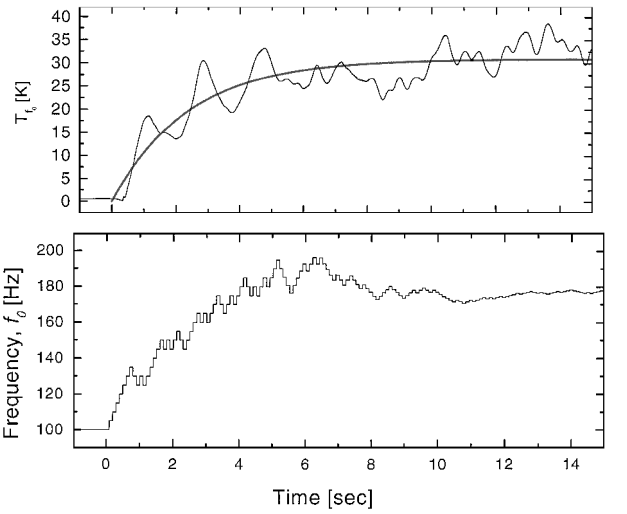

Fig. 11 Overall time response of the second control strategy, which adjusted the forcing frequency (bottom panel) to maximize the temperature oscillations at the forcing frequency. Maximum step size was 5 Hz, and minimum step size was 0.5 Hz.

Second Control Strategy

The objective of the second control strategy was to optimize the forcing frequency in addition to the phase and amplitude. A variable-step hill-climbing algorithm was used to shift the forcing frequency every 100 ms to maximize the magnitude of the temperature oscillations. To avoid being trapped in the local minima of the complicated performance surface of Fig. 6, large initial step sizes were used (5 Hz). The step size was then slowly reduced to allow the algorithm to settle on a maximum. This approach is similar in principle to simulated annealing.[29]

The performance of the second control strategy is shown in Fig. 11 for the C_2H_4–N_2 mixture. The initial frequency was set at 100 Hz. After 5 s, the step size was reduced (by 5% every iteration) until the minimum step size of 0.5 Hz was reached. This control strategy typically converged in approximately 10 s.

The phase optimization algorithm of the first strategy was expected to operate independently of the frequency optimization algorithm. However during the first 5–10 ms after a change in the frequency, the desired oscillations were at a different frequency than the measured oscillations because the combustor had not yet responded to the new frequency. This would trigger a large phase shift as the controller attempted to compensate, i.e., 5 Hz is equivalent to a phase shift of 1.8 deg/ms. Although the typical phase error was less than 20 deg, this interference could be mitigated by either delaying the switch of the frequency in the temperature decomposition algorithm and the desired response or suspending the LMS adaptation until a few characteristic flow times had passed (10–15 ms).

The small step size of the converged second strategy (0.5 Hz) will allow the control system to track a slowly varying maximum. However, there are situations where a nearby local maximum would result in lower CO emissions. Because the convergence time of the second strategy was similar to the flow-through time of the fast-sampling cell, an improved control strategy might incorporate the CO measurements to determine whether to reset the step size of the frequency searching algorithm to 5 Hz and allow the control system to search nearby maxima for an improved forcing frequency. Additionally, in a real combustor measurements of CO and unburned hydrocarbons could aid the determination of the appropriate amount of supplemental fuel injection or excess air addition for optimization of the equivalence ratio, and the temperature measurements could be used to detect flame instability and insufficient combustion temperature.

Conclusions

A computer-controlled closed-loop feedback system that incorporates a multiplexed diode-laser absorption sensor was demonstrated to monitor and control the magnitude of forced temperature

oscillations (T_{rms} values) in the combustion region of a 50-kW pulsed incinerator. In addition, measurements of CO, C_2H_2, and C_2H_4 concentrations in exhaust gases were recorded using a fast-sampling probe and a multipass cell. The feedback system was applied to maximize measured T_{rms} values and thus increase the coherence of temperature oscillations by adjusting the relative phase angle between the primary and secondary air forcing. Effective feedback control of T_{rms} substantially reduced the measured CO, C_2H_2, and C_2H_4 concentrations in the exhaust.

The feedback control system could be improved by identifying and actively suppressing higher-order modes in the combustor and by incorporating adaptive logic that would anticipate frequency shifts of these modes. Finally, the overall burner performance could be improved further by using, in addition to measured temperature values, measured CO and C_2H_4 concentrations and pressure in an advanced, comprehensive closed-loop strategy.

The successful demonstration of closed-loop control in a realistic combustion system illustrates the high potential of diode-laser absorption sensors for improved measurement and control of combustion and other high-temperature process streams, particularly for applications that require remote and nonintrusive monitoring.

Acknowledgments

This research was supported by the Strategic Environmental Research and Development Program with K. Schadow as Technical Monitor and the U.S. Air Force Office of Scientific Research, Aerospace Sciences and Materials Directorate, with J. Tishkoff as Technical Monitor. Both the assistance of T. P. Parr with the experiments and the donation of a detector from New Focus, Inc., are gratefully acknowledged.

References

[1]Philippe, L. C., and Hanson, R. K., "Laser Diode Wavelength-Modulation Spectroscopy for Simultaneous Measurement of Temperature, Pressure, and Velocity in Shock-Heated Oxygen Flows," *Applied Optics*, Vol. 32, No. 30, 1993, pp. 6090–6103.

[2]Arroyo, M. P., Birbeck, T. P., Baer, D. S., and Hanson, R. K., "Dual Diode-Laser Fiber-Optic Diagnostic for Water-Vapor Measurements," *Optics Letters*, Vol. 19, No. 14, 1994, pp. 1091–1093.

[3]Baer, D. S., Nagali, V., Furlong, E. R., Hanson, R. K., and Newfield, M. E., "Scanned- and Fixed-Wavelength Absorption Diagnostics for Combustion Measurements Using Multiplexed Diode Lasers," *AIAA Journal*, Vol. 34, No. 3, 1996, pp. 489–493.

[4]Allen, M. G., and Kessler, W. J., "Simultaneous Water Vapor Concentration and Temperature Measurements Using 1.31-μm Diode Lasers," *AIAA Journal*, Vol. 34, No. 3, 1996, pp. 483–488.

[5]Miller, M. F., Kessler, W. J., and Allen, M. G., "Diode Laser-Based Air Mass Flux Sensor for Subsonic Aeropropulsion Inlets," *Applied Optics*, Vol. 35, No. 24, 1996, pp. 4905–4912.

[6]Silver, J. A., Kane, D. J., and Greenberg, P. S., "Quantitative Species Measurements in Microgravity Flames Using near-IR Diode Lasers," *Applied Optics*, Vol. 34, No. 15, 1995, pp. 2787–2801.

[7]Nagali, V., Furlong, E. R., Chou, S. I., Mihalcea, R. M., Baer, D. S., and Hanson, R. K., "Diode-Laser Sensor System for Multi-Species and Multi-Parameter Measurements in Combustion Flows," AIAA Paper 95-2684, July 1995.

[8]Baer, D. S., Hanson, R. K., Newfield, M. E., and Gopaul, N. K. L. M., "Multiplexed Diode-Laser Sensor System for Simultaneous H_2O, O_2 and Temperature Measurements," *Optics Letters*, Vol. 19, No. 22, 1994, pp. 1900–1902.

[9]Parr, T. P., Gutmark, E. J., Wilson, K. J., Hanson-Parr, D. M., Yu, K., Smith, R. A., and Schadow, K. C., "Compact Incinerator Afterburner Concept Based on Vortex Combustion," *Twenty-Sixth Symposium (International) on Combustion*, Combustion Inst., Pittsburgh, PA, 1996, pp. 2471–2477.

[10]Parr, T. P., Wilson, K. J., Yu, K., Smith, R. S., and Schadow, K. C., "Actively Controlled Afterburner for Compact Waste Incinerator," *Proceedings of the 1996 International Conference on Incineration and Thermal Treatment Technologies*, Office of Environment, Health, and Safety, Univ. of California, Irvine, CA, 1996, pp. 787–793.

[11]Cole, J. A., Hansell, D. W., Widmer, N. C., and Seeker, W. R., "Forced Acoustic Field Effects on Incineration Processes: Research on U.S. Navy Shipboard Waste Disposal," Spring Meeting of the Western States Section of the Combustion Inst., Paper 97S-043, Livermore, CA, April 1997.

[12]Widrow, B., and Stearns, S. D., *Adaptive Signal Processing*, Prentice–Hall, Englewood Cliffs, NJ, 1985.

[13]Haykin, S., *Adaptive Filter Theory*, Prentice–Hall, Englewood Cliffs, NJ, 1996.

[14]McManus, K. R., Magill, J. C., Miller, M. F., and Allen, M. G., "Combustion Instability Suppression in Liquid-Fueled Combustors," AIAA Paper 97-0463, Jan. 1997.

[15]Brouwer, J., Ault, B. A., Bobrow, J. E., and Samuelson, G. S., "Active Control for Gas Turbine Combustors," *Twenty-Third Symposium (International) on Combustion*, Combustion Inst., Pittsburgh, PA, 1990, pp. 1087–1092.

[16]Padmanabhan, K. T., Bowman, C. T., and Powell, J. D., "Adaptive Optimal Combustion Control Strategy," *Combustion and Flame*, Vol. 100, No. 1–2, 1995, pp. 101–110.

[17]McManus, K. R., Poinsot, T., and Candel, S. M., "Review of Active Control of Cumbustion Instabilities," *Progress in Energy and Combustion Science*, Vol. 19, No. 1, 1993, pp. 1–29.

[18]Billoud, G., Galland, M. A., Huu, C. H., and Candel, S., "Adaptive Active Control of Cumbustion Instabilities," *Combustion Science and Technology*, Vol. 81, 1992, pp. 257–283.

[19]Neumeier, Y., and Zinn, B. T., "Experimental Demonstration of Active Control of Combustion Instabilities Using Real-Time Modes Observation and Secondary Fuel Injection," *Twenty-Sixth Symposium (International) on Combustion*, Combustion Inst., Pittsburgh, PA, 1996, pp. 2811–2818.

[20]Kemal, A., and Bowman, C. T., "Real-Time Adaptive Feedback Control of Combustion Instability," *Twenty-Sixth Symposium (International) on Combustion*, Combustion Inst., Pittsburgh, PA, 1996, pp. 2803–2809.

[21]Furlong, E. R., Mihalcea, R. M., Webber, M. E., Baer, D. S., Hanson, R. K., and Parr, T. P., "Diode-Laser Sensor System for Closed-Loop Control of a 50-kW Incinerator," *SPIE's Optical Technology in Fluid, Thermal, and Combustion Flows III*, Vol. 3172, 1997, pp. 324–330.

[22]Eckbreth, A. C., *Laser Diagnostics for Combustion Temperature and Species*, Gordon and Breach, Amsterdam, The Netherlands, 1996.

[23]Toth, R. A., "Extensive Measurements of $H_2^{16}O$ Frequencies and Strengths: 5750 to 7965 cm^{-1}," *Applied Optics*, Vol. 33, No. 21, 1994, pp. 4851–4867.

[24]Rothman, L. S., Gamache, R. R., Tipping, R. H., Rinsland, C. P., Smith, M. A. H., Benner, D. C., Devi, V. M., Flaud, J.-M., Camay-Peyret, C., Perrin, A., Goldman, A., Massie, S. T., Brown, L. R., and Toth, R. A., "The HITRAN Molecular Database: Editions of 1991 and 1992," *Journal of Quantitative Spectroscopy and Radiative Transfer*, Vol. 48, No. 5–6, 1992, pp. 469–507.

[25]Mihalcea, R. M., Baer, D. S., and Hanson, R. K., "Diode Laser Sensor for Measurements of CO, CO_2, and CH_4 in Combustion Flows," *Applied Optics*, Vol. 36, No. 33, 1997, pp. 8745–8752.

[26]Furlong, E. R., Baer, D. S., and Hanson, R. K., "Combustion Control Using a Multiplexed Diode-Laser Sensor," *Twenty-Sixth Symposium (International) on Combustion*, Combustion Inst., Pittsburgh, PA, 1996, pp. 2851–2858.

[27]Furlong, E. R., Baer, D. S., and Hanson, R. K., "Combustion Control and Monitoring Using a Multiplexed Diode-Laser Sensor System," AIAA Paper 96-2763, July 1996.

[28]Furlong, E. R., Mihalcea, R. M., Webber, M. E., Baer, D. S., and Hanson, R. K., "Combustion Sensing and Control Using Wavelength-Multiplexed Diode Lasers," AIAA Paper 97-0320, Jan. 1997.

[29]Kirkpatrick, S., Gelatt, C. D., and Vecchi, M. P., "Optimization by Simulated Annealing," *Science*, Vol. 20, No. 4598, 1983, pp. 671–680.

R. P. Lucht
Associate Editor